A synthetic approach for enhanced thermoelectric properties of PEDOT:PSS bulk composites

Kaya Wei, Troy Stedman, Zhen-Hua Ge, Lilia M. Woods,[a] and George S. Nolas[a]
Department of Physics, University of South Florida, Tampa, Florida 33620, USA

(Received 23 June 2015; accepted 1 October 2015; published online 15 October 2015)

The thermoelectric properties of PEDOT:PSS/$Bi_{0.5}Sb_{1.5}Te_3$ polymer/inorganic bulk composites with different $Bi_{0.5}Sb_{1.5}Te_3$ content were investigated. The composites were prepared at various concentrations of $Bi_{0.5}Sb_{1.5}Te_3$ by a solution-phase process before grinding to fine powders in liquid N_2 for hot pressing into bulk polymer composite materials. The measured transport properties are well described within a theoretical model for effective media involving a tunneling mechanism induced by thermal voltage fluctuations. Our results present a strategy for the preparation of bulk polymer composites and demonstrate an avenue for optimization of the thermoelectric properties of PEDOT:PSS/$Bi_{0.5}Sb_{1.5}Te_3$ bulk composites. © *2015 AIP Publishing LLC*.
[http://dx.doi.org/10.1063/1.4933254]

Recently, polymers have been considered for thermoelectric applications primarily because of their unique combination of properties that are atypical of inorganic material, namely, mechanical flexibility, low cost, low temperature and low cost processing, and general non-toxicity.[1–3] Polymers typically possess a relatively low thermal conductivity, κ, at room temperature.[4] In addition, tuning the electrical conductivity by several orders of magnitude is possible in conducting polymers,[5,6] which may result in a reduced Seebeck coefficient, S.[7,8] The thermoelectric properties[9] of polymers are therefore relatively less desirable for thermoelectrics applications as compared to that of inorganic semiconductors.

A decrease in the electrical resistivity, ρ, of PEDOT:PSS can be realized with the addition of polar solvents such as ethylene glycol (EG) or dimethylsulfoxide (DMSO).[10–13] Although the exact mechanism for this is still unresolved, the use of polar solvents to reduce ρ in PEDOT:PSS has been demonstrated[14] and resulted in improved thermoelectric performance, with power factors ($PF = S^2/\rho$) that exceed 10 μW/m K^2.[2] Carbon nanotubes,[6,15] Te nanotubes,[1,16] and Bi_2Te_3 plates[17] have all been used as the inorganic component in polymer/inorganic film composites. The ρ values of these composite films were readily reduced, however a different outcome resulted when attempting to optimize S.[1,6,15–17] Nevertheless, the very low κ for polymer materials remains, even in composites containing carbon nanotubes that possess relatively high κ values.[6]

Conducting polymer/inorganic nanoparticle composite films have also been investigated due to their ease of preparation, resulting in improved thermoelectric properties.[1–5] Nevertheless, the difficulty in measuring the thermoelectric properties of films[18] as well as applying such knowledge to bulk thermoelectric devices[9] still remains. The governing transport mechanisms in polymers are also very different than that of crystalline matter. Upon doping, the π-bonding along the polymer chains coupled with disorder and dopant counterions can lead to the formation of polarons. Heat and charge conduction are therefore facilitated by hopping between polaron sites.[19] For highly doped conducting polymers, localized conducting regions can be formed for which tunneling induced by thermal voltage fluctuations becomes important, as shown initially for tunneling conductivity.[20] While the theory of polaron hopping has been developed by several authors,[21,22] only recently has a complete transport model for fluctuation-induced tunneling becomes available.[23] An investigation targeting the underlying experimental and theoretical aspects of bulk conducting polymers is therefore of great interest.

In this work, we report on the thermoelectric properties of polymer/inorganic bulk composites of PEDOT:PSS/$Bi_{0.5}Sb_{1.5}Te_3$ with different $Bi_{0.5}Sb_{1.5}Te_3$ concentrations and demonstrate enhanced thermoelectric properties as a result of our investigation. In addition, we present an approach for the fabrication of bulk polymer composites. By mixing PEDOT:PSS with $Bi_{0.5}Sb_{1.5}Te_3$ using an ultrasonic bath and grinding the resulting polymer composite into fine powders in liquid N_2 in order to densify them into bulk homogeneous materials by employing hot pressing, bulk PEDOT:PSS/$Bi_{0.5}Sb_{1.5}Te_3$ composites can be processed. This approach is very efficient in producing bulk polymer/inorganic composites with the inorganic contents uniformly dispersed in the composite and therefore is of interest for both scientific research and industrial applications. Enhanced thermoelectric properties are achieved through this approach, as will be discussed below. In addition, calculated transport properties utilizing our recently developed linear response theory for thermal voltage fluctuations tunneling are compared with the measured data. The role of the tunneling characteristics and the overall performance of the composites are then analyzed to identify possible routes for enhanced thermoelectric performance.

For the preparation of our polymer/inorganic bulk composites, Poly(3,4-ethylenedioxythiophene)-poly(styrenesulfonate) (PEDOT:PSS, 3%–4% in water) was purchased from ALORICH and used without further processing. A $Bi_{0.5}$ $Sb_{1.5}Te_3$ alloy ingot, obtained from Marlow Industries, Inc., was ground to fine powder (400 mesh) before mixing

[a]lmwoods@usf.edu and gnolas@usf.edu

with PEDOT:PSS in an ultrasonic bath for 4 h. The mixture was then dried at 35 °C for 12 h forming PEDOT:PSS/$Bi_{0.5}Sb_{1.5}Te_3$ pieces. The polymer composite pieces were then ground to fine powders in liquid nitrogen followed by drying under vacuum for 12 h. For densification, the PEDOT:PSS/$Bi_{0.5}Sb_{1.5}Te_3$ fine powders were hot pressed into pellets using custom-designed 12 mm diameter graphite tooling at 45 MPa and 100 °C for 1 h. The densities of the 0 wt. % $Bi_{0.5}Sb_{1.5}Te_3$, 30 wt. %, 60 wt. %, and 90 wt. % specimens are 2.8 g/cm^3, 3.9 g/cm^3, 4.7 g/cm^3, and 5.9 g/cm^3, respectively. The theoretical density of each specimen was achieved given the fact that the density of PEDOT:PSS is 1.3 g/cm^3 (dry coating) and $Bi_{0.5}Sb_{1.5}Te_3$ is 6.6 g/cm^3. After hot pressing, a scanning electron microscope (SEM, JEOL JSM-6390LV) was used to image the specimens and observe the relative distribution of the polymer and inorganic material, while XRD data were collected using a Bruker D8 Advance diffractometer with DAVINCI design equipped with a Lynxeye detector using Cu Ka radiation. The densified pellets were cut into 2 mm × 2 mm × 7 mm parallelepipeds for temperature dependent four-probe ρ, S (gradient sweep method), and steady-state κ measurements from 45 K to 300 K. The measurements were conducted in a custom radiation-shielded vacuum probe with uncertainties of 4%, 6%, and 8% for ρ, S, and κ measurements, respectively.[24]

The composites basically consist of many large conducting regions beyond the percolation limit, thus the transport is mainly due to tunneling between the formed junctions (Figure 1(e)). The tunneling process in such systems is affected by the thermal voltage fluctuations from the excess or deficit charges across the junction[20,23,25] which create a local thermal field, $\mathcal{E}_T$, in addition to the external field $\mathcal{E}$. There is, in effect, a parallel plate capacitor with probability $P(\mathcal{E}_T) = \left(\frac{2\varepsilon_0 wA}{\pi k_B T}\right)^{1/2} e^{\left(-\varepsilon_0 wA\mathcal{E}_T^2/2k_B T\right)}$ for generating $\mathcal{E}_T$, where w is the width of the junction, A is the overlap area between the conducting regions, ε_0 is the permittivity between the conducting region, T is the temperature, and k_B is Boltzmann's constant.[20,23] The transport is further characterized using an effective medium theory[26,27] for an inhomogeneous system, assuming that the composite can be represented by a medium with average junction parameters (Figure 1(f)). The tunneling charge (j) and heat (j^q) currents are determined using a Landauer-type theory for carriers with energy $E = \frac{\hbar^2 k^2}{2m}$ (m is the effective mass, $\boldsymbol{k}$ is the wave vector) which are also thermally averaged over all possible $\mathcal{E}_T$. The currents are given as

$$j = \frac{qm}{2\pi^2\hbar^3}\int_0^\infty dE[f_R(E,\mu_R,T_R) - f_L(E,\mu_L,T_L)]\int_0^E D(F,E_x)dE_x, \tag{1}$$

$$j^Q_{L,R} = \frac{qm}{2\pi^2\hbar^3}\int_0^\infty dE[f_R(E,\mu_R,T_R) - f_L(E,\mu_L,T_L)] \times [E-\mu_{L,R}]\int_0^E D(F,E_x)dE_x, \tag{2}$$

where the integration is from the bottom of the conduction band, q is the carrier charge, j^Q_L and j^Q_R refer to the heat current into the left reservoir and out of the right reservoir, respectively, $f_R(E,\mu_R,T_R)$ and $f_L(E,\mu_L,T_L)$ are the Fermi distribution functions, and $\mu_{L,R}$ are the Fermi levels of the left and right reservoirs, respectively (Figure 1(f)). $D(F,E)$ is the carrier tunneling probability for a net electric field $F = \mathcal{E} \pm \mathcal{E}_T$ and refers to the fluctuation-induced field $\mathcal{E}_T$ pointing to the right (+) with $\mu_L = \mu - qw(\mathcal{E}_T + \mathcal{E})$ and $\mu_R = \mu$ or the left (−) with $\mu_L = \mu$ and $\mu_R = \mu - qw(\mathcal{E}_T - \mathcal{E})$. Since there are two equally probable orientations of $\mathcal{E}_T$, the total currents through the junction for a given $\mathcal{E}_T$ are

$$J = \frac{1}{2}[j(\mathcal{E}+\mathcal{E}_T,\nabla T) + j(\mathcal{E}-\mathcal{E}_T,\nabla T)], \tag{3}$$

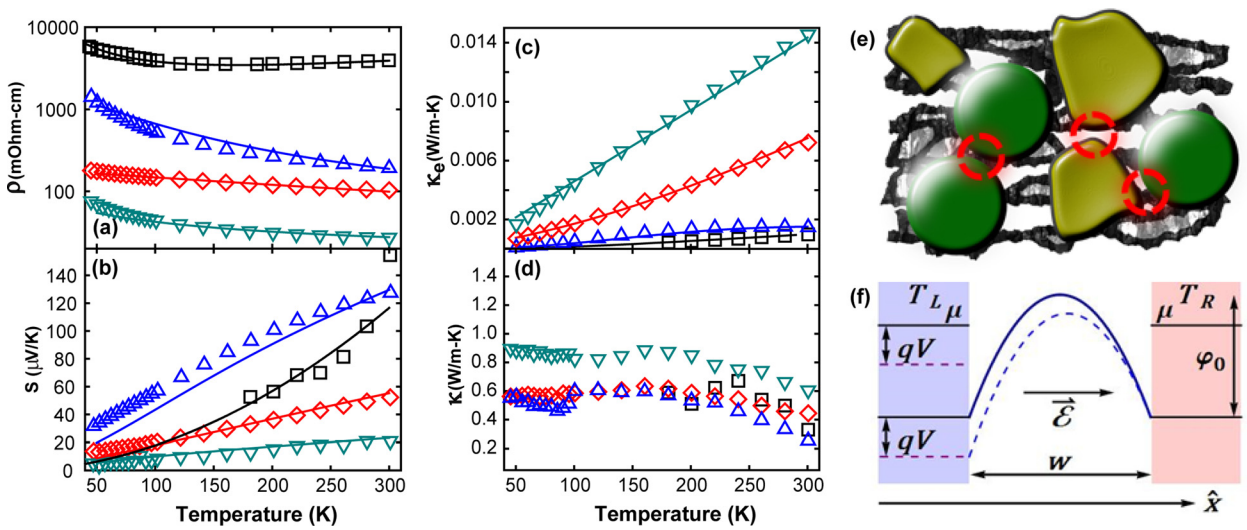

FIG. 1. Temperature dependent (a) ρ, (b) S, (c) κ_E, and (d) κ of PEDOT:PSS/$Bi_{0.5}Sb_{1.5}Te_3$ composites with a $Bi_{0.5}Sb_{1.5}Te_3$ content of 0 wt. % (square), 30 wt. % (up triangle), 60 wt. % (diamond), and 90 wt. % (down triangle). The solid lines are the calculated values. For the 0 wt. % specimen, the theoretical curve was calculated from the procedure described in this work and outlined in Ref. 23. (e) A schematic representation of a polymer composite with $Bi_{0.5}Sb_{1.5}Te_3$ inclusions (green) and conducting regions (yellow) formed on the chains of the polymers (black). The formed tunneling junctions (circled in red) are taken into account within an effective medium theory. (f) The average tunneling junction of width w is described by a parabolic barrier of height φ_0 between the two regions of temperatures $T_L < T_R$ with (dashed) and without (solid) an electric field $\vec{\mathcal{E}}$. The Fermi level μ and the conduction band minimum are lowered on the left by an amount qV by the electric field.

$$J^Q = \frac{1}{4}\left[j_L^Q(\mathcal{E}+\mathcal{E}_T,\nabla T) + j_L^Q(\mathcal{E}-\mathcal{E}_T,\nabla T) + j_R^Q(\mathcal{E}+\mathcal{E}_T,\nabla T) + j_R^Q(\mathcal{E}-\mathcal{E}_T,\nabla T)\right]. \quad (4)$$

The carrier transport properties are obtained using linear response theory followed by thermal averaging over the probability $P(\mathcal{E}_T)$.[28]

Figures 1(a) and 1(b) show the temperature dependent ρ and S of the PEDOT:PSS/$Bi_{0.5}Sb_{1.5}Te_3$ composites with a $Bi_{0.5}Sb_{1.5}Te_3$ content of 0, 30, 60, and 90 wt. %. Over the entire measured temperature range ρ decreases with increasing $Bi_{0.5}Sb_{1.5}Te_3$ content, as shown in Figure 1(a), while ρ of PEDOT:PSS is not very temperature dependent, especially above 100 K, although the composites show a decrease in ρ with increasing temperature. The S values at room temperature, as shown in Figure 1(b), decrease with increasing $Bi_{0.5}Sb_{1.5}Te_3$ content, consistent with the ρ behavior. Due to the difficulty in stabilizing the temperature gradient at low temperatures, S for PEDOT:PSS was only measured to 180 K, however, our calculations (solid line in Figure 1(b)) show S to lower temperatures.

The theoretical calculations based on the fluctuation-induced tunneling mechanism (Eqs. (1)–(4)) are shown as solid lines in Figure 1. We used a parabolic function for the energy barrier $\varphi(x) = \begin{cases} 4\varphi_0 \frac{x}{w^2}(w-x) - qV\frac{(w-x)}{w}, & 0 \le x \le w \\ 0, & otherwise, \end{cases}$ and the tunneling probability $D(F,E_x)$ is calculated via the WKB approximation. The effective parameters for each composite are given in Table I. Figures 1(a) and 1(b) show very good agreement with the measured data. Our calculations also show how the balance between μ and m evolves as the $Bi_{0.5}Sb_{1.5}Te_3$ content increases, and account for the decrease in ρ with increasing $Bi_{0.5}Sb_{1.5}Te_3$ content. It is interesting to note that even though ρ for the 30 wt. % composite is smaller than that for pure PEDOT:PSS, the S values have the opposite trend below room temperature. Transport property variations in polymer composites are in general strongly influenced by their morphology.[5–8] Morphology changes can be attributed to various factors, including types of surfactants used, chemical changes in the polymers due a particular type of carrier doping, and modifications in interfacial regions facilitating tunneling transport. Here, the interfacial polymer/$Bi_{0.5}Sb_{1.5}Te_3$ regions are an important source for the particular morphology in the different specimens. SEM results suggest that the incorporation of $Bi_{0.5}Sb_{1.5}Te_3$ causes distortion of the polymer matrix.[28] The 30 wt. % specimen naturally contains the lowest amount of inorganic regions of our three composites due to the fact that it had the lowest $Bi_{0.5}Sb_{1.5}Te_3$ content. Previous reports also show that morphology can affect transport significantly, including changing the transport properties by orders of magnitude for the same type of polymer.[8,19,25]

Figures 1(c) and 1(d) show κ for the PEDOT:PSS/$Bi_{0.5}Sb_{1.5}Te_3$ composites with the electronic contribution, κ_E, shown in Figure 1(c). The calculated κ_E agrees well with our estimated κ_E ($=L_0T/\rho$) using the calculated L_0 values employing the Wiedemann-Franz relation (L_0 is the Lorentz number). The κ_E values increase with higher $Bi_{0.5}Sb_{1.5}Te_3$ content as expected, however, κ_L is the dominant contribution ($\kappa = \kappa_E + \kappa_L$) for all specimens due to their high ρ values. Above 200 K and below 300 K, the composites with 30 and 60 wt. % $Bi_{0.5}Sb_{1.5}Te_3$ content achieved lower κ values as compared with that of PEDOT:PSS due to the high density of disordered regions in the polymer chain alignment when forming a composite with $Bi_{0.5}Sb_{1.5}Te_3$.[29] In the case of the 90 wt. % $Bi_{0.5}Sb_{1.5}Te_3$ content specimen, with the highest density of disordered regions, PEDOT:PSS acts as a barrier separating the conducting $Bi_{0.5}Sb_{1.5}Te_3$ domains. This results in higher κ values over the measured temperature range.[25] Nevertheless, relatively low κ values, preferable for good thermoelectrics, are shown in all specimens due to the intrinsic properties of PEDOT:PSS.[30]

Temperature dependent PF and ZT values for all specimens are shown in Figures 2(a) and 2(b). The room temperature PF for the 30 wt. % $Bi_{0.5}Sb_{1.5}Te_3$ specimen is an order of magnitude higher than that for the PEDOT:PSS specimen. The PF of our PEDOT:PSS, also densified using hot pressing, is higher than that of cold pressed PEDOT:PSS[31] suggesting that hot pressing is more effective in densifying the polymer composites. The room temperature PF of the 30 wt. % $Bi_{0.5}Sb_{1.5}Te_3$ specimen is comparable to that of other PEDOT:PSS/Bi_2Te_3 composites.[7] As is the case in

TABLE I. Parameters used in the theoretical fits to the experimental data.

Specimen	w (nm)	A (nm^2)	φ_0 (eV)	m/m_0	μ (eV)
PEDOT:PSS	15.57	0.37	1.7	0.001	…
30 wt. % $Bi_{0.5}Sb_{1.5}Te_3$	2.8	5.0	0.41	0.21	0.27
60 wt. % $Bi_{0.5}Sb_{1.5}Te_3$	3.0	11	1.18	0.1	0.82
90 wt. % $Bi_{0.5}Sb_{1.5}Te_3$	3.0	1.0	1.8	0.06	1.42

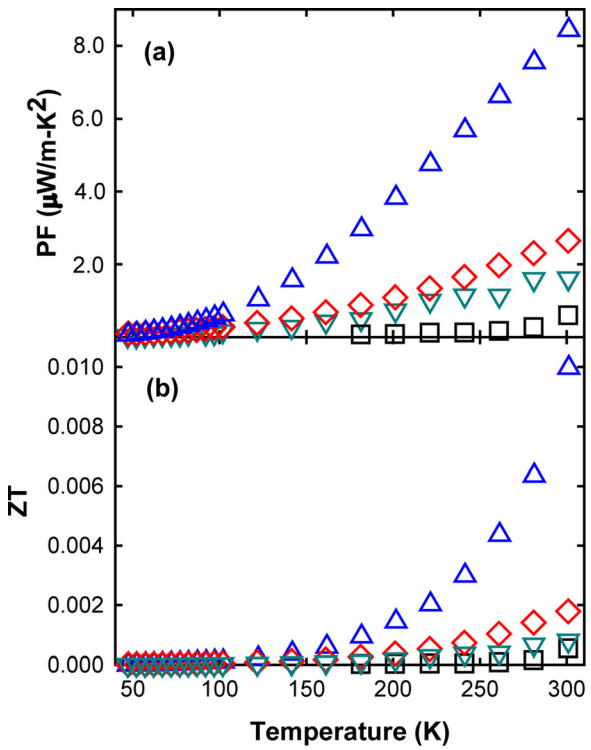

FIG. 2. Temperature dependent PF (a) and ZT (b) of PEDOT:PSS/$Bi_{0.5}Sb_{1.5}Te_3$ composites. The symbols corresponding to each specimen are as defined in Figure 1.

investigations of other polymer/inorganic materials,[7,8] the higher content of the thermoelectric material in our composites will greatly reduce *S* resulting in a lower *PF* for the 60 and 90 wt. % specimens as compared with that of the 30 wt. % specimen. For this reason, the highest *ZT* corresponds to the specimen with a 30 wt. % $Bi_{0.5}Sb_{1.5}Te_3$ content because of the high *PF* together with a low κ. The enhanced *ZT* values for the bulk PEDOT:PSS/$Bi_{0.5}Sb_{1.5}Te_3$ composites compared with that of the PEDOT:PSS coupled with our synthetic method suggest an approach for further investigating and optimizing the thermoelectric properties of polymer/inorganic composites in bulk form for improved thermoelectric properties.

An approach was reported for the preparation and densification of PEDOT:PSS/$Bi_{0.5}Sb_{1.5}Te_3$ bulk composites resulting in improved thermoelectric properties as compared with pristine PEDOT:PSS. The interfacial regions formed by the organic/inorganic interfaces are key in enhancing the thermoelectric properties of composites over that of the pure polymer, similar in approach to that of nanostructured materials and core-shell inclusions.[32–34] Theoretical calculations based on fluctuation-induced tunneling are in excellent agreement with our experimental results and show that the fluctuation-induced tunneling model applies to thermoelectric transport in these materials. This agreement is indicative of transport in polymers governed by mechanisms typically not present in crystalline materials. The room temperature *ZT* for the PEDOT:PSS/$Bi_{0.5}Sb_{1.5}Te_3$ 30 wt. % composite is almost two orders-of-magnitude higher than that of PEDOT:PSS. These results describe an approach for polymer bulk materials research.

This work was supported by the National Science Foundation under Contract No. DMR-1400957. K.W. acknowledges support by the II–VI Foundation Block-Gift Program. We thank Dr. J. Sharp of Marlow Industries, Inc. for the $Bi_{0.5}Sb_{1.5}Te_3$ alloy thermoelectric material.

[1]M. He, F. Qiu, and Z. Q. Lin, Energy Environ. Sci. **6**, 1352 (2013).
[2]Y. Du, S. Z. Shen, K. Cai, and P. S. Casey, Prog. Polym. Sci. **37**, 820 (2012).
[3]N. Dubey and M. Leclerc, J. Polym. Sci., Part B: Polym. Phys. **49**, 467 (2011).
[4]C. Yu, K. Choi, L. Yin, and J. C. Grunlan, ACS Nano **5**, 7885 (2011).
[5]M. H. Harun, E. Saion, A. Kassim, N. Yahya, and E. Mahmud, JASA **2**, 63 (2007).
[6]C. Bounioux, P. Diaz-Chao, M. Campoy-Quiles, M. S. Martin-Gonzalez, A. R. Goni, R. Yerushalmi-Rozen, and C. Muller, Energy Environ. Sci. **6**, 918 (2013).
[7]H. J. Song, C. C. Liu, H. F. Zhu, F. F. Kong, B. Y. Lu, J. K. Xu, J. M. Wang, and F. Zhao, J. Electron. Mater. **42**, 1268 (2013).
[8]S. K. Yee, N. E. Coates, A. Majumdar, J. J. Urban, and R. A. Segalman, Phys. Chem. Chem. Phys. **15**, 4024 (2013).
[9]G. S. Nolas, J. W. Sharp, and H. J. Goldsmid, *Thermoelectrics: Basics Principles and New Materials Developments* (Springer-Verlag, Berlin, 2001).
[10]J. Ouyang, Q. Xu, C.-W. Chu, Y. Yang, G. Li, and J. Shinar, Polymer **45**, 8443 (2004).
[11]Y. J. Xia and J. Y. Ouyang, J. Mater. Chem. **21**, 4927 (2011).
[12]O. P. Dimitriev, Y. P. Piryatinski, and A. A. Pud, J. Phys. Chem. B **115**, 1357 (2011).
[13]X. Crispin, F. L. E. Jakobsson, A. Crispin, P. C. M. Grim, P. Andersson, A. Volodin, C. V. Haesendonck, M. Van der Auweraer, W. R. Salaneck, and M. Berggren, Chem. Mater. **18**, 4354 (2006).
[14]Y. H. Kim, C. Sachse, M. L. Machala, C. May, L. Muller-Meskamp, and K. Leo, Adv. Funct. Mater. **21**, 1076 (2011).
[15]H. Song, C. Liu, J. Xu, Q. Jiang, and H. Shi, RSC Adv. **3**, 22065 (2013).
[16]Y. M. Sun, P. Sheng, C. A. Di, F. Jiao, W. Xu, D. Qiu, and D. B. Zhu, Adv. Mater. **24**, 932 (2012).
[17]M. He, J. Ge, Z. Q. Lin, X. H. Feng, X. W. Wang, H. B. Lu, Y. L. Yang, and F. Qiu, Energy Environ. Sci. **5**, 8351 (2012).
[18]G.-H. Kim, L. Shao, K. Zhang, and K. P. Pipe, Nat. Mater. **12**, 719 (2013).
[19]O. Bubnova and X. Crispin, Energy Environ. Sci. **5**, 9345 (2012).
[20]P. Sheng, Phys. Rev. B **21**, 2180 (1980).
[21]N. F. Mott and E. A. Davis, *Electronic Processes in Non-Crystalline Materials*, 2nd ed. (Clarenton, Oxford, 1979).
[22]H. Overhof, Phys. Status Solidi B **67**, 709 (1975).
[23]T. Stedman, K. Wei, G. S. Nolas, and L. M. Woods, "Thermoelectricity in polymer composites due to fluctuation-induced tunneling," Chem. Phys. Chem (to be published).
[24]J. Martin, G. S. Nolas, H. Wang, and J. Yang, J. Appl. Phys. **99**, 044903 (2006).
[25]A. B. Kaiser, Adv. Mater. **13**, 927 (2001).
[26]S. Kirkpatrick, Rev. Mod. Phys. **45**, 574 (1973).
[27]I. Webman, J. Jortner, and M. Cohen, Phys. Rev. B **16**, 2959 (1977).
[28]See supplementary material at http://dx.doi.org/10.1063/1.4933254 for details of the thermal voltage fluctuations induced tunneling model, XRD, and SEM results.
[29]P. J. Phillips, Rep. Prog. Phys. **53**, 549 (1990).
[30]A. Weathers, Adv. Mater. **27**, 2101 (2015).
[31]F. X. Jiang, J. K. Xu, B. Y. Lu, Y. Xie, R. J. Huang, and L. F. Li, Chin. Phys. Lett. **25**, 2202 (2008).
[32]J. Martin, L. Wang, L. Chen, and G. S. Nolas, Phys. Rev. B **79**, 115311 (2009).
[33]A. Popescu, L. M. Woods, J. Martin, and G. S. Nolas, Phys. Rev. B **79**, 205302 (2009).
[34]B. Liao, M. Zebarjadi, K. Esfarjani, and G. Chen, Phys. Rev. Lett. **109**, 126806 (2012).